Effect of Complementary Hydrogen Bonding Additives in Subphase on the Structure and Properties of the 2-Amino-4,6-dioctadecylamino-1,3,5-triazine Amphiphile at the Air−Water Interface: Studies by Ultraviolet−Visible Absorption Spectroscopy and Brewster Angle Microscopy

Qun Huo, K. C. Russell,* and Roger M. Leblanc*

Department of Chemistry, University of Miami, P.O. Box 249118, Coral Gables, Florida 33124

Received December 3, 1997. In Final Form: February 10, 1998

The present work is focused on the effects of hydrogen bonding on the 2-D properties of aminotriazine amphiphile **1** ($2C_{18}$TAZ) by incorporating different complementary hydrogen bonding components in the subphase. The structural organization of **1** at the air−water interface in the presence of barbituric acid (BA), barbital (BT), and cyanuric acid (CA) was examined by surface pressure−area isotherm measurements, Ultraviolet-visible (UV−vis) absorption spectroscopy, and Brewster angle microscopy. UV−vis absorption spectra reveal that amphiphile **1** forms an irreversible monolayer at the air−water interface due to its "auto assembly". The binding of BA molecules to a $2C_{18}$TAZ monolayer can be detected by UV spectra at BA subphase concentrations as low as 0.01 mM. Different complementary hydrogen bonding additives in the subphase have different effects on the monolayer structure and properties of **1**, which are likely due to the different structures of hydrogen bonding additives at the air−water interface. The effects of organic solvents in the subphase was also investigated. The strong solvating ability of dimethyl sulfoxide (DMSO) destroyed the hydrogen bonding network whereas dioxane enhanced the hydrogen bonding between **1** and its hydrogen bonding complements.

Introduction

Molecular recognition is a key concept in chemistry and life sciences. The use of multiple hydrogen bonding as a means of specific recognition has attracted enormous interest from chemists and biochemists.[1−9] From the double helical structure, the replication and transcription of DNA, to the highly efficient catalytic activity of most enzymes, hydrogen bonding plays an extremely important role in biological systems. For synthetic chemists, the highly selective and directional nature of the hydrogen bond provides an important tool in the construction and stabilization of large noncovalently linked molecular and supramolecular architectures. Recently, the self-assembly of triaminopyrimidines (TAP) or triaminotriazines (TAZ) with complementary barbiturate or cyanurate components has been the focus of active investigation.[8,10−18] With change of the steric substituent groups in triazines or barbiturates, three motifs have been observed in the crystalline state for these assemblies, linear ribbons or tapes, crinkled tapes, and supramolecular macrocycles or rosettes. These studies may result in the design of new molecular electronic devices or molecular materials.[19−22]

Since most of the biological molecular recognition processes occur in aqueous media or at the interface of cell membranes, the study of the hydrogen bonding assisted molecular recognition at the air−water interface has become an important research area for biochemists and surface chemists.[23] Monolayers with hydrophilic groups, such as diaminotriazines, urea, orotate, Kemp's acid, peptides, guanidinium, or resorcinol groups, have been found to bind to polar substrates including nucleobases, nitrogen aromatics, amino acids, peptides, AMP, ATP, and sugars from the aqueous subphase efficiently.[24−38] Molecular recognition at the air−water

* To whom correspondence may be addressed at the University of Miami. Tel: 305-284-2282 (or 6856). Fax: 305-284-4571. E-mail: MMODRONO@umiami.ir.miami.edu.

(1) Rebek, J., Jr.; Nemeth, D. *J. Am. Chem. Soc.* **1986**, *108*, 5637.
(2) Rebek, J., Jr. *Acc. Chem. Res.* **1990**, *23*, 399.
(3) Chang, S.-K.; Van Engen, D.; Fan, E.; Hamilton, A. D. *J. Am. Chem. Soc.* **1991**, *113*, 7640.
(4) Hamilton, A. D.; Van Engen, D. *J. Am. Chem. Soc.* **1987**, *109*, 5035.
(5) Aoyama, Y.; Tanaka, Y.; Toi, H.; Ogoshi, H. *J. Am. Chem. Soc.* **1988**, *110*, 634.
(6) Aoyama, Y.; Tanaka, Y.; Sugahara, S. *J. Am. Chem. Soc.* **1989**, *111*, 5397.
(7) Lehn, J.-M. *Pure Appl. Chem.* **1994**, *66*, 1961.
(8) Russell, K. C.; Leize, E.; Van Dorsselaer, A.; Lehn, J.-M. *Angew. Chem., Int. Ed. Engl.* **1995**, *34*, 209−213.
(9) Marsh, A.; Nolen, E. G.; Gardinier, K. M.; Lehn, J.-M. *Tetrahedron Lett.* **1994**, *35*, 397.
(10) Zerkowski, J. A.; Seto, C. T.; Weirda, D. A.; Whitesides, G. M. *J. Am. Chem. Soc.* **1990**, *112*, 9025−9026.
(11) Zerkowski, J. A.; Seto, C. T.; Whitesides, G. M. *J. Am. Chem. Soc.* **1992**, *114*, 5473−5475.
(12) Seto, C. T.; Whitesides, G. M. *J. Am. Chem. Soc.* **1993**, *115*, 905−916.
(13) Zerkowski, J. A.; Whitesides, G. M. *J. Am. Chem. Soc.* **1994**, *116*, 4298−4304.
(14) Zerkowski, J. A.; Mcdonald, J. C.; Seto, C. T.; Wierda, D.; Whitesides, G. M. *J. Am. Chem. Soc.* **1994**, *116*, 2382−2391.
(15) Zerkowski, J. A.; Mathias, J. P.; Whitesides, G. M. *J. Am. Chem. Soc.* **1994**, *116*, 5305−4315.
(16) Zerkowski, J. A.; McDonald, J. C.; Whitesides, G. M. *Chem. Mater.* **1994**, *6*, 1250−1257.
(17) Mathias, J. P.; Simanek, E. E.; Zerkowski, J. A.; Seto, C. T.; Whitesides, G. M. *J. Am. Chem. Soc.* **1994**, *116*, 4316−4325.
(18) Mathias, J. P.; Seto, C. T.; Simanek, E. E.; Whitesides, G. M. *J. Am. Chem. Soc.* **1994**, *116*, 1725−1736.
(19) Lehn, J. M. *Angew. Chem., Int. Ed. Engl.* **1990**, *29*, 1304−1319.
(20) Whitesides, G. M.; Mathias, J. P.; Seto, C. T. *Science* **1991**, *254*, 1312−1319.
(21) Lehn, J. M. *Makromol. Chem., Macromol. Symp.* **1993**, *69*, 1−17.
(22) Hartgerink, J. D.; Granja, J. R.; Milligan, R. A.; Ghadiri, M. R. *J. Am. Chem. Soc.* **1996**, *118*, 43−50.
(23) Paleous, C. M.; Tsiourvas, D. *Adv. Mater.* **1997**, *9*, 695−710.
(24) Ikeura, Y.; Kurihara, K.; Kunitake, T. *J. Am. Chem. Soc.* **1991**, *113*, 7342−7350.
(25) Sasaki, D. Y.; Kurihara, K.; Kunitake, T. *J. Am. Chem. Soc.* **1991**, *113*, 9685−9686.

S0743-7463(97)01329-2 CCC: $15.00
Published on Web 03/18/1998

interface has been recently reported by other groups as well.[39−44] This specific molecular recognition could be useful for future technology, for example, in creating new chemical or biosensors and in construction of molecular lattices comprising multiple functional units for molecular devices in two-dimensions.[45]

More specifically, the molecular recognition of two complementary hydrogen bonding components, barbiturates and TAZs or TAPs at the air−water interface, has been recently studied by Kunitake's and Rinsdorf's groups. In Kunitake's works,[46] diaminotriazine functionalized amphiphiles were synthesized to form stable monolayers at the air−water interface. Combined examination using Fourier transform infrared (FTIR), ESCA and reflection absorption spectroscopy confirmed specific binding of barbituric acid and thiobarbituric acid to the monolayer due to hydrogen bonding between the diaminotriazine head of the amphiphiles and the imide moiety of the barbiturates. However the amphiphiles were not designed to form a complementary hydrogen bonding network with barbiturates. Later, atomic force microscopy (AFM) was used to observe a monolayer of 2-amino-4,6-didodecylamino-1,3,5-triazine ($2C_{12}$TAZ) transferred from barbituric acid solution onto a mica plate which showed regularly arrayed terminal methyl groups of the triazine amphiphile as a result of hydrogen-bond networking with barbituric acid.[47] Furthermore, the steric effects of hydrophobic alkyl groups on the properties of melamine amphiphiles has been investigated.[48] Aqueous barbituric acid and amphiphiles bearing two or three alkyl chains formed a 1:1 alternating network structure whereas *N*,*N*,*N*′,*N*′-tetrasubstituted melamine amphiphiles formed 2:1 (BA/amphiphile) complexes. In contrast, Ringsdorf's work has focused on studying the different binding modes of TAP and urea as substrates to barbituric acid lipids by in situ FTIR and UV−vis reflection spectroscopy.[40,41,49] TAP can form six hydrogen bonds while urea can only form four hydrogen bonds with barbituric acid lipids. The catalytic effect of TAP on the hydrolysis of barbituric acid lipids at the air−water interface has also been investigated by surface pressure−area isotherm studies and UV−Vis absorption spectroscopy.

As mentioned earlier, TAZs can form different hydrogen bonding networks, i.e., linear tapes, crinkled tapes, or rosettes with barbiturates, cyanuric acid, or isocyanurates by changing the substituent groups in these compounds. No literature has been published on the similar studies at the air−water interface. It is our objective to compare the binding behavior of different barbiturates and cyanuric acid to the TAZ amphiphile monolayers, hoping to bring more information about the formation of these 1:1 hydrogen bonding networks at the air−water interface. As a start, 2-amino-4,6-dioctadecylamino-1,3,5-triazine (**1,** $2C_{18}$TAZ) (Chart 1) was synthesized as a model amphiphile surfactant. Three complementary hydrogen bonding components were chosen as subphase additives due to their unique structural characteristics: barbituric acid **2** (BA), barbital **3** (BT), and cyanuric acid **4** (CA) (Chart 1). All three compounds can form six-point hydrogen bonding complementary with two triazine amphiphiles as shown. Compared to BA, BT bears two ethyl groups. We expect to see some changes between these two components due to the steric or hydrophobic effects of the two ethyl groups. As for CA, because it is a C_3 symmetrical molecule, possessing three symmetrical hydrogen donor−acceptor−donor faces, it should affect the structure of hydrogen bonding network in a different way from BT and BA.

Polar solvents such as dimethyl sulfoxide (DMSO) disrupt the binding of complementary hydrogen bonding components due to the strong solvation of hydrogen-bond donor sites, whereas nonpolar solvents such as dioxane enhance the formation of hydrogen bonding at the air−water interface due to its poor solvation ability. Therefore, the addition of a small amount of DMSO or dioxane to the aqueous subphase should change the structure and properties of **1** monolayer. These changes would further confirm that the formation of the highly organized structures at the air−water interface is due to complementary hydrogen bonding.

The use of highly sensitive UV−vis absorption spectroscopy directly at the air−water interface to study the binding of complementary hydrogen bonding components in subphase to monolayers has been also investigated in this work. Also for the first time, Brewster angle microscopy was employed to study the TAZ monolayer topography. It was expected that the formation of hydrogen bonding networks at the air−water interface due to the presence of additives in the subphase would bring about specific changes to the TAZ monolayer morphologies.

Experimental Section

Materials. Octadecylamine (98%), barbituric acid (99%), and cyanuric acid (98%) were purchased from Aldrich Chemical Co. and used in organic synthesis or monolayer studies directly. Barbital was purchased from Sigma Chemical Co. (St. Louis, MO) as crystalline solid. All organic solvents for the synthesis

(26) Kurihara, K.; Ohto, K.; Tanaka, Y.; Aoyama, Y.; Kunitake, T. *J. Am. Chem. Soc.* **1991**, *113*, 444−450.
(27) Sasaki, D. Y.; Kurihara, K.; Kunitake, T. *J. Am. Chem. Soc.* **1992**, *114*, 10994−10995.
(28) Kawahara, T.; Kurihara, K.; Kunitake, T. *Chem. Lett.* **1992**, 1839−1842.
(29) Taguchi, K.; Ariga, K.; Kunitake, T. *Chem. Lett.* **1995**, 701−702.
(30) Oishi, Y.; Torii, Y.; Kuramori, M.; Suehiro, K.; Ariga, K.; Taguchi, K.; Kamino, A.; Kunitake, T. *Chem. Lett.* **1996**, 411−412.
(31) Cha, X.; Ariga, K.; Kunitake, T. *J. Am. Chem. Soc.* **1996**, *118*, 9545−9551.
(32) Oishi, Y.; Kato, T.; Kuramori, M.; Suehiro, K.; Ariga, K.; Kamino, A.; Koyano, H.; Kunitake, T. *Chem. Lett.* **1996**, 857−858.
(33) Onda, M.; Yoshihara, K.; Koyano, H.; Ariga, K.; Kunitake, T. *J. Am. Chem. Soc.* **1996**, *118*, 8524−8530.
(34) Cha, X.; Ariga, K.; Kunitake, T. *Bull. Chem. Soc. Jpn.* **1996**, *69*, 163−168.
(35) Kamino, A.; Koyano, H.; Ariga, K.; Kunitake, T. *Bull. Chem. Soc. Jpn.* **1996**, *69*, 3619−3631.
(36) Oishi, Y.; Kato, T.; Kuramori, M.; Suehiro, K.; Ariga, K.; A., K.; Koyano, H.; Kunitake, T. *J. Chem. Soc., Chem. Commun.* **1997**, 1357−1358.
(37) Ariga, K.; Kamino, A.; Koyano, H.; Kunitake, T. *J. Mater. Chem.* **1997**, *7*, 1155−1161.
(38) Oishi, Y.; Torii, Y.; Kato, T.; Kuramori, M.; Suehiro, K.; Ariga, K.; Taguchi, K.; Kamino, A.; Koyano, H.; Kumitake, T. *Langmuir* **1997**, *13*, 519−524.
(39) Kitano, H.; Ringsdorf, H. *Bull. Chem. Soc. Jpn.* **1985**, *58*, 2826.
(40) Bohanon, T. M.; Denzinger, S.; Fink, R.; Paulus, W.; Ringsdorf, H.; Weck, M. *Angew. Chem., Int. Ed. Engl.* **1995**, *34*, 58−60.
(41) Ahuja, R.; Caruso, P. L.; Möbius, W. P.; Ringsdorf, H.; Wildburg, G. *Angew. Chem., Int. Ed. Engl.* **1993**, *32*, 1033−1036.
(42) Chai, X. C.; Chen, S. G.; Zhou, Y. L.; Zhao, Y. Y.; Li, T. J.; Lehn, J.-M. *Chin. J. Chem.* **1995**, *13*, 385.
(43) Shimomura, M.; Karthause, O.; Ijiro, K. *Supramol. Sci.* **1996**, *3*, 61.
(44) Ebara, Y.; Itakura, K.; Okahata, Y. *Langmuir* **1996**, *12*, 5165.
(45) Kurihara, K. *Colloids Surf., A: Physicochem. Eng. Aspects* **1997**, *123−124*, 425−432.
(46) Honda, Y.; Kurihara, K.; Kunitake, T. *Chem. Lett.* **1991**, 681−684.
(47) Koyano, H.; Yoshihara, K.; Ariga, K.; Kunitake, T.; Oishi, Y.; Kawano, O.; Kuramori, M.; Suehiro, K. *J. Chem. Soc., Chem. Commun.* **1996**, 1769−1770.
(48) Koyano, H.; Bissel, P.; Yoshihara, K.; Ariga, K.; Kunitake, T. *Chem. Eur. J.* **1997**, *3*, 1077−1082.
(49) Weck, M.; Fink, R.; Ringsdorf, H. *Langmuir* **1997**, *13*, 3515−3522.

Chart 1. Structures of 2-Amino-4,6-dioctadecylamino-1,3,5-triazine ($2C_{18}$TAZ) Amphiphile (1), Complementary Hydrogen Bonding. Components Barbituric acid (BA) (2), Barbital (BT) (3), Cyanuric acid (CA) (4), and an Illustration of Six-Point Hydrogen Bonding between 1 and 2

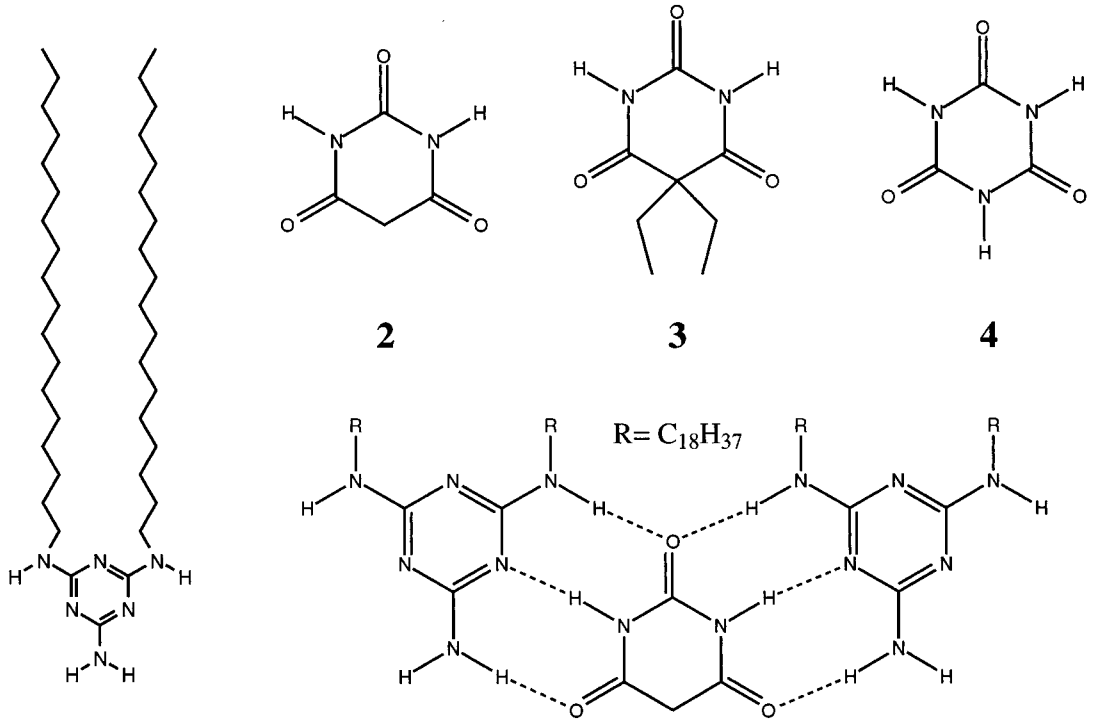

and purification were purchased from Fisher Scientific Co. as reagent grade and were used without further purification. 2-Amino-4,6-dichloro-1,3,5-triazine was prepared from cyanuric chloride and anhydrous ammonia according to the literature.[14] The ^{1}H NMR spectra were obtained from a Varian VXR 400 MHz spectrometer. The mass spectrum was recorded on a VG-Trio 2000 mass spectrometer. The combustion analysis was conducted by Atlantic Microlab Inc. (Norcross, GA). The melting point was obtained from a Thomas-Hoover melting point apparatus and uncorrected.

Synthesis and Characterization of 2-Amino-4,6-dioctadecylamino-1,3,5-triazine (1, $2C_{18}$TAZ). To the solution of 2-amino-4,6-dichloro-1,3,5-triazine (2.0 g, 12 mmol) in acetone (15 mL), octadecylamine (6.75 g, 25 mmol) was added portionwise. Under vigorous stirring, saturated aqueous sodium carbonate (1.6 g, 15 mmol) was added dropwise. The reaction mixture was brought to reflux overnight. After cooling to room temperature, the reaction mixture was filtered, and the solid was washed with a few portions of acetone and hot water and then vacuum-dried. The crude product was further purified by crystallization from hot hexane with a yield of 75% as white crystal. Mp 98−101 °C. ^{1}H NMR ($CDCl_3$): 0.85−1.75 (m, 70H), 3.3 (b, 4H), 4.7 (b, 4H). FAB MS: calcd 630.63, found 631.52 (M^+). Anal. Calcd for $C_{39}H_{78}N_6$ (631.09): C, 74.23; H, 12.46; N, 13.32. Found: C, 74.08; H, 12.47; N, 13.05.

General Methods for Monolayer Studies. HPLC grade chloroform was obtained from Fisher Scientific Co. The dimethyl sulfoxide (DMSO) and dioxane used in the subphase are also HPLC grade from Aldrich Chemical Co. Pure $2C_{18}$TAZ was dissolved in chloroform to a concentration of 1.0 mM. The water used for the monolayer study was purified by a Modulab 2020 water purification system (Continental Water Systems Corp., San Antonio, TX). The water has a resistance of 18 MΩ·m and a surface tension of 72.6 mN/m at 20 °C. The pH values of all the subphases were measured with an Accumet model 10 pH meter from Fisher Scientific Co. before use. For the subphase of pure water, 10 mM BA, 10 mM BT, 10 mM CA, 1 mM BA, 0.01 mM BA, 10 mM BA in 10% DMSO/water (v/v), 10 mM BA in 20% DMSO/water (v/v), 10 mM CA in 10% DMSO/water (v/v), 10 mM CA in 10% dioxane (v/v), the pH value were 5.70, 2.82, 4.80, 3.85, 3.45, 4.70, 2.91, 2.80, 4.42, and 4.42, respectively. All surface tensions were measured by a digital-tensionmeter, model K10 (KRÜSS GmbH Wissenschaftliche Labogeräte, Hamburg, Germany). The injected volume of the $2C_{18}$TAZ solution (1.0 mM) was 35 μL for the surface pressure−area isotherm measurements and 50 μL for the Brewster angle experiments. After the sample was spread, a 10 min period was allowed to pass for the complete evaporation of solvent before compression. The compression rate was set up at 12 mm/min for all experiments.

All the experiments were conducted in a clean room class 1000 where the temperature (20 ± 1 °C) and the humidity (50 ± 1%) are controlled. Two different Langmuir troughs were used. The Langmuir trough used for the surface pressure measurements was a KSV minitrough. Two computer-controlled symmetrically movable barriers were used to regulate the surface area. The trough dimensions were 7.5 cm × 30 cm. The surface pressure was measured by the Wilhelmy method. The sensitivity of the Wilhelmy plate is ±0.01 mN/m. All the isotherm measurements were repeated three times, and the isotherm presented is the average of three measurements. The difference between the average isotherm and any of the three individual isotherms is ±1 Å^2/molecule. A UV−vis spectrophotometer (Hewlett-Packard Co., Wilmington, DE) can be slid over the KSV trough for recording the absorption spectra of a $2C_{18}$TAZ monolayer directly at the air/water interface at different surface pressures.

For the Brewster angle measurements, a Nippon trough (5 cm × 47 cm), equipped with a moving wall system (NL-LB140S-MWC, Nippon Laser & Electronics Lab., Nagoya, Japan) was used, to which was connected a Brewster angle microscope (BAM) (EMM633S, Nippon Laser & Electronics Lab., Nagoya, Japan), a helium−neon laser (wavelength 632.8 nm and power 10 mW), and a CCD camera. The images from the CCD were captured and digitized using a digital video capture mode (Snappy video Snapshot, Rancho Cordova, CA) for further analysis. The surface morphology of the $2C_{18}$TAZ monolayers in different subphases was visualized and recorded during the compression by using the BAM. The images were analyzed at different surface pressures using the digital video capture mode mentioned above. The three-dimensional (3D) representations of the BAM images were also investigated using a software NIH 1.62 image that allowed noise reduction using a low-pass filter. The dark areas of the image are translated by low peaks whereas the bright area

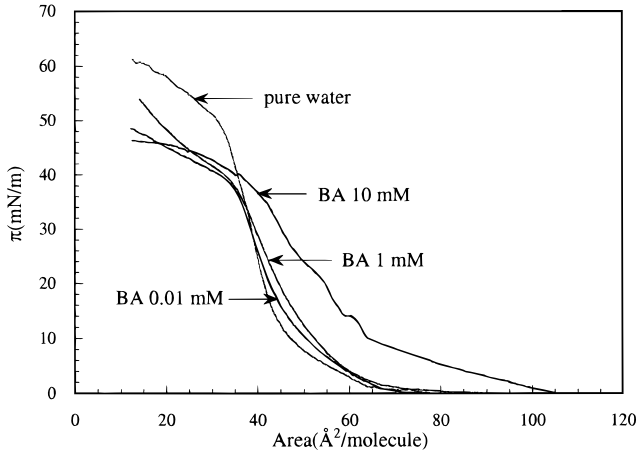

Figure 1. Surface pressure−area isotherms of $2C_{18}$TAZ with different concentrations of barbituric acid (BA) as subphase.

represent high peaks in the 3D figures. All the images presented in this work have dimensions of 400 μm × 400 μm.

Results

Surface Pressure−Area Isotherms of a $2C_{18}$TAZ Monolayer in a Pure Water Subphase and Barbituric Acid Subphase at Different Concentrations. The $\pi-A$ isotherm of $2C_{18}$TAZ in pure water shows that this dialkylamine amphiphile has a liquid condensed phase between surface pressure of 2 and 15 mN/m and a solid phase between 15 and 45 mN/m on pure water subphase (Figure 1). The limiting molecular area, 47.5 Å^2/molecule, is practically identical to the calculated 50.4 Å^2/molecule.[50] With the presence of BA in subphase the $\pi-A$ isotherms behave differently at various concentrations. At 10 mM BA subphase, the $\pi-A$ isotherm shows an obviously increased molecular area at the same surface pressure, larger area at the initial rising point, slopes with lower gradients, and a decreased collapse surface pressure. With the decreasing BA concentration in the subphase, the difference is not as apparent. For 0.01 mM BA, the isotherm is very close to the isotherm on the pure water subphase. The limiting areas obtained from 10, 1, and 0.01 mM BA subphases are approximately 70.0, 55.5, and 49.0 Å^2/molecule, respectively. All these results suggest the binding of BA in the subphase to the $2C_{18}$TAZ monolayer. The $2C_{18}$TAZ monolayer swelled with increasing concentration of BA.

Comparison of $\pi-A$ Isotherms of the $2C_{18}$TAZ Monolayer with Various Complementary Hydrogen Bonding Components at a Concentration of 10 mM in the Subphase. Figure 2 shows the different effect of 10 mM BA, BT, and CA in subphase on the $\pi-A$ isotherm of the $2C_{18}$TAZ monolayer. Compared to the $\pi-A$ isotherm on pure water, the BA subphase brought up apparent changes as previously stated. In the case of the BT subphase, the slope keeps the same gradient, but the molecular area at the initial rising point lower down to the point which is only slightly higher than the one from the pure water subphase. The collapse surface pressure is further decreased. At the same surface pressure, the molecular area increases only slightly. The limiting area from this $\pi-A$ isotherm is ∼58 Å^2/molecule. As for the CA subphase, the changes are unusual: both the area at the initial rising point and the molecular area at same surface pressure decreased. This is exactly the opposite of the isotherms generated from BA and BT subphases, yet the collapse surface pressure is decreased as was observed from BA and BT subphases. The limiting molecular area obtained is about 50.0 Å^2/molecule.

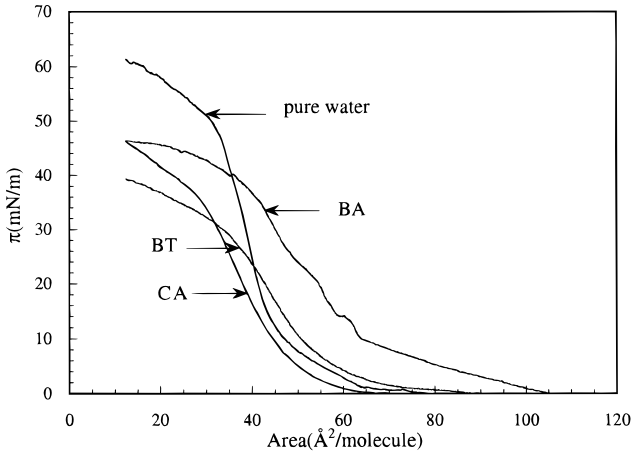

Figure 2. Surface pressure−area isotherms of the $2C_{18}$TAZ monolayer with different complementary hydrogen bonding additives, i.e., BA, BT, and CA in the subphase at a concentration of 10 mM.

Effect of DMSO and Dioxane in the Subphase on the Surface Pressure−Area Isotherm of the $2C_{18}$TAZ Monolayer. Figure 3a shows the $\pi-A$ isotherms of a $2C_{18}$TAZ monolayer on a water subphase containing various percentages of DMSO and dioxane. On the 10% DMSO/water and 20% DMSO/water subphase the $\pi-A$ isotherm did not show much change. Only a slightly lower collapse pressure was observed. However, with the addition of 10% dioxane in the water subphase, the molecular area was slightly decreased at the same surface pressure, which suggests a more tightly packed monolayer structure. The collapse surface pressure also decreased under these conditions. Figure 3b shows the effect of 10% DMSO and 20% DMSO in water on the $\pi-A$ isotherm of a $2C_{18}$TAZ monolayer in a 10 mM BA subphase. With increasing DMSO concentration the $\pi-A$ isotherm becomes more like the $\pi-A$ isotherm from the pure water subphase. First, the initial rising point approaches that in pure water. Second, the molecular area at the same surface pressure does not increase as much as was found from the BA subphase without DMSO. These analyze clearly indicate that the hydrogen bonding network formed from the BA subphase and $2C_{18}$TAZ at the air−water interface is partially disrupted by DMSO. Figure 3c compares the effect of 10% DMSO versus 10% dioxane in the CA subphase on the $2C_{18}$TAZ monolayer $\pi-A$ isotherms. Even though the changes are small, the difference between subphases containing DMSO and dioxane can still be distinguished. The $\pi-A$ isotherm in 10% DMSO was nearly indistinguishable from the isotherm in its absence, whereas 10% dioxane caused a decreased molecular area at the same surface pressure, indicating a more tightly packed monolayer. In this case the collapse surface pressure also decreased more as compared to the CA subphase without dioxane.

UV−vis Absorption Spectroscopic Study of $2C_{18}$TAZ Monolayer and the Binding of BA in Subphase to the Monolayer. Figure 4a shows the UV spectra of a $2C_{18}$TAZ monolayer recorded at different surface pressures during compression. With increasing surface pressure, the absorption band of a $2C_{18}$TAZ monolayer at 220 nm increased. After the surface pressure reached ∼15

(50) Structures were calculated using software MacroModel (Version 5.5, University of Columbia), with Amber* force field on a Silicon Graphics Indigo II computer. Mohamadi, F.; Richards, N. G. J.; Guida, W. C.; Liskamp, R.; Lipton, M.; Caufield, C.; Chang, G.; Hendrickson, T.; Still, W. C. *J. Comput. Chem.* **1990**, *11*, 440−467.

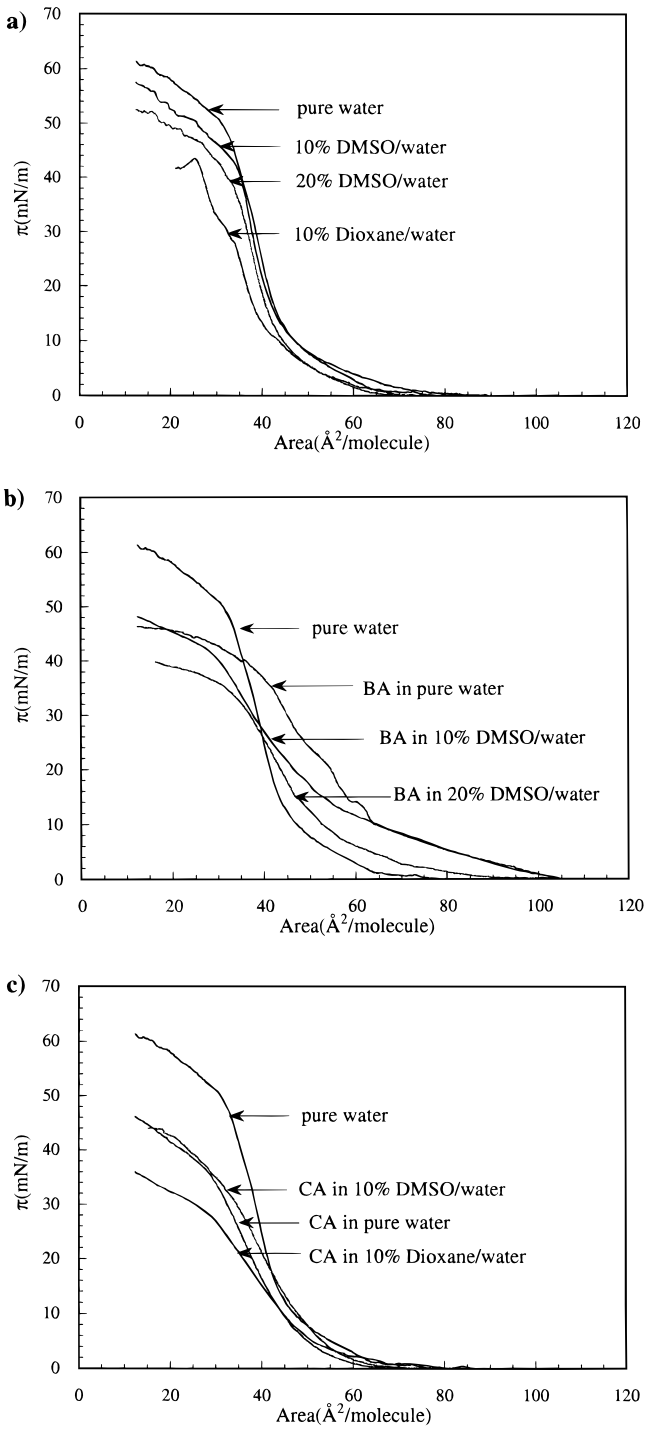

Figure 3. Effect of different percentages of DMSO or dioxane dissolved in the subphase on the surface pressure−area isotherms of $2C_{18}$TAZ monolayer: (a) water; (b) BA 10 mM; (c) CA 10 mM.

mN/m, the absorbance did not increase significantly with further compression. This indicates the formation of a well-packed $2C_{18}$TAZ monolayer at a surface pressure of about 15 mN/m, in agreement with the $\pi-A$ isotherm measurement. The reversibility of a $2C_{18}$TAZ monolayer was also examined by UV spectroscopy as shown in Figure 4b. When the surface pressure reached 15 mN/m, the barrier was stopped and moved back to maximum molecular area. The absorbance of the $2C_{18}$TAZ monolayer did not return to the original value at surface pressure 0 mN/m. Instead, it maintained the value measured at 15 mN/m, even after waiting for 1 h. The surface pressure of the monolayer only decreased slightly during this time. These results strongly suggest the formation of an irreversible network at the air−water interface due to interactions between $2C_{18}$TAZ molecules. We were also hoping to use UV absorption to study the binding of BA molecules in the subphase to the $2C_{18}$TAZ monolayer. Unfortunately, as shown in Figure 4c, the absorption of the BA subphase is too high even at 1 mM. As a result, we were not able to observe the $2C_{18}$TAZ monolayer absorption band at the air−water interface. However, the binding of BA in the 0.01 mM BA subphase to the $2C_{18}$TAZ monolayer was clearly detectable through the direct observation of the BA absorption band at the air−water interface (Figure 4d). The bathochromic shift of maximum absorption for BA molecules from 259 to 269 nm confirms the complexation of BA molecules to the $2C_{18}$-TAZ monolayer. For the BT and CA subphase, because their UV absorption bands overlap with $2C_{18}$TAZ monolayer absorption band, no UV spectra are presented.

Brewster Angle Microscopy (BAM) Study of the $2C_{18}$TAZ Monolayer in Different Subphases. The surface morphologies of the $2C_{18}$TAZ monolayer under the addition of different complementary hydrogen bonding components in subphase have been studied by Brewster angle microscopy images at two surface pressures during the compression. First the BAM images (shown in left column) and their 3-D representations (shown in right column) of $2C_{18}$TAZ monolayer in the pure water subphase was compared to the images obtained from BA (10 mM), BT (10 mM), and CA (10 mM) subphases, respectively (Figure 5). In pure water, the $2C_{18}$TAZ monolayer shows a smooth, tightly packed, and uniform structure at both surface pressures, 15 and 30 mN/m (Figure 5a). In contrast, the images from the BA subphase are full of short, bright strips which are distributed randomly on the surface at surface pressures of 20 and 30 mN/m (Figure 5b). From their 3-D representations we see more clearly the random islands with different depths "floating" on the water surface. This is in agreement with the rough shape of its $\pi-A$ isotherm. With BT as an additive in the subphase, at surface pressure of 15 mN/m (Figure 5c), a plain surface with some randomly scattered bright areas is seen. However, the brightness is much less intense than the images from BA subphase which means lower molecular density at the air−water interface. The 3-D representation confirms this difference. With the increase of surface pressure to 30 mN/m (Figure 5c), there comes the accumulation of some bright areas with an approximate long strip boundary along the vertical direction. These long strips seem to be formed from the tight packing of many short strips which run horizontally along the image. In summary, compared to the images from the BA subphase, the surface morphology of the $2C_{18}$TAZ monolayer in the BT subphase seems much smoother and the brightness decreased a lot. In the case of CA subphase, at surface pressure of 20 mN/m, some short strips with varying brightness are observed in the images (Figure 5d). By comparison with the images from the BA subphase, these strips are much more orderly located. Their 3-D representations clearly show the strips running horizontally along the images. With the surface pressure increased to 30 mN/m (Figure 5d), the trend of the formation of long strips becomes more apparent and the brightness of these strips increased, which indicates an increased molecular density.

Figure 6 shows the effect of 20% DMSO in water on the BAM images of a $2C_{18}$TAZ monolayer in BA subphase. At a surface pressure of 20 mN/m, a more uniform and smooth monolayer structure is observed with the addition of 20%

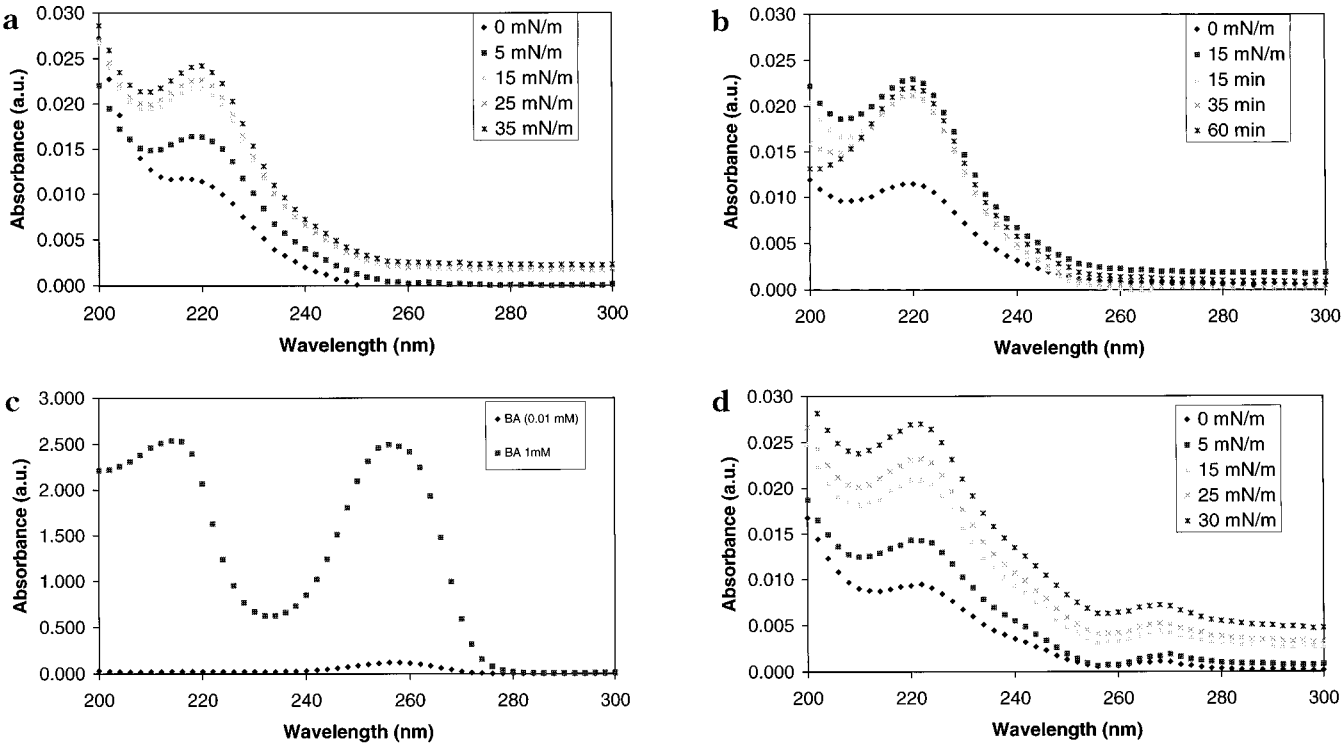

Figure 4. (a) UV spectra of the $2C_{18}$TAZ monolayer at different surface pressures. (b) UV spectra of $2C_{18}$TAZ monolayer taken at different times after the barrier was moved back from 15 mN/m to the largest molecular area available. Note: a nil surface pressure was not observed at the end of the decompression, i.e., moving the barrier back to its original position before compression. (c) UV spectra of BA at two different concentrations. (d) UV spectra of the $2C_{18}$TAZ monolayer with 0.01 mM BA subphase at different surface pressures.

DMSO as compared to the surface morphology of a $2C_{18}$-TAZ monolayer without the addition of DMSO (Figure 5b). The brightness also decreased significantly implying a decreased molecular density. With the surface pressure increased to 30 mN/m, even though there also comes the formation of bright short strips, these strips are much more evenly distributed on the surface instead of being scattered randomly as in the case without the addition of DMSO.

Figure 7 shows the different effects of 10% DMSO and 10% dioxane in CA subphase on the $2C_{18}$TAZ monolayer BAM images. The difference is very distinct. With the addition of 10% DMSO (Figure 7a), the surface becomes much more plain and unwavering and the brightness decreased a lot, with no obvious intense local tight packing. In contrast, with the addition of 10% dioxane (Figure 7b), the formation of many unevenly scattered island structures is seen at both surface pressures of 15 and 30 mN/m. Even though the "strip" shape of the islands can still be distinguished, compared to the images without the addition of dioxane, the outline is more blurred and the size of the bright areas is obviously increased.

Discussion

The Structure and Property of $2C_{18}$TAZ Monolayer in Pure Water. Without any addition of complementary hydrogen bonding components to the subphase, the $\pi-A$ isotherm shows the formation of a well-packed $2C_{18}$TAZ monolayer structure with a limiting area of 47.5 Å^2/molecule, which is very close to the MacroModel calculation result 50.4 Å^2/molecule.[50] However, as its UV spectra in parts a and b of Figure 4 show, $2C_{18}$TAZ forms an irreversible network during the compression. Since the $2C_{18}$TAZ triazine headgroup contains both hydrogen bonding donors and acceptors, it is very likely the $2C_{18}$-TAZ molecules "autoassemble" at the air−water interface by hydrogen bonding. Since only one type of molecule exists at the air−water interface, the formation of a hydrogen bonding network is homogeneous, and this explains why the surface morphology looks very plain, no obvious local domains were observed (Figure 5a). It seems impossible for the $2C_{18}$TAZ molecule to use all six hydrogen bonding sites to form a self-complementary hydrogen bonded network. Two- or four-point hydrogen bonding is more feasible. This partially formed hydrogen bonding network is much weaker than a heterocomplementary hydrogen bonded network. Even though it was pointed out that it is possible for triaminopyrimidine molecules to "autoassemble" without the presence of any other assemblers in the solid state,[51] this has never been demonstrated in solution. At the air−water interface, during the compression of monolayer, the $2C_{18}$TAZ molecules start to gather together in a highly ordered pattern: with the long hydrophobic chain floating in the air and the triazine headgroup in the subphase. When the distance between these headgroups is short enough, a weak yet irreversible hydrogen bonding network is formed. The experimental limiting area for a $2C_{18}$TAZ molecule obtained from the isotherm (47.5 Å^2/molecule) is lower than the theoretical value (50.4 Å^2/molecule), which is not usual. In Kunitake's paper,[48] the limiting molecular area for the $2C_{12}$TAZ molecule obtained from $\pi-A$ isotherm is ∼42.0 Å^2/molecule, which is also lower than the theoretical value (50.2 Å^2/molecule).[50] These results can be explained by the formation of weakly hydrogen bonded network between dialkylTAZ molecules at the air−water interface. The $2C_{18}$TAZ molecules are more tightly packed than expected when no hydrogen bonding effect is considered.

(51) Lehn, J. M.; Mascal, M.; DeCien, A.; Fischer, J. *J. Chem. Soc., Chem. Commun.* **1990**, *6*, 479−481.

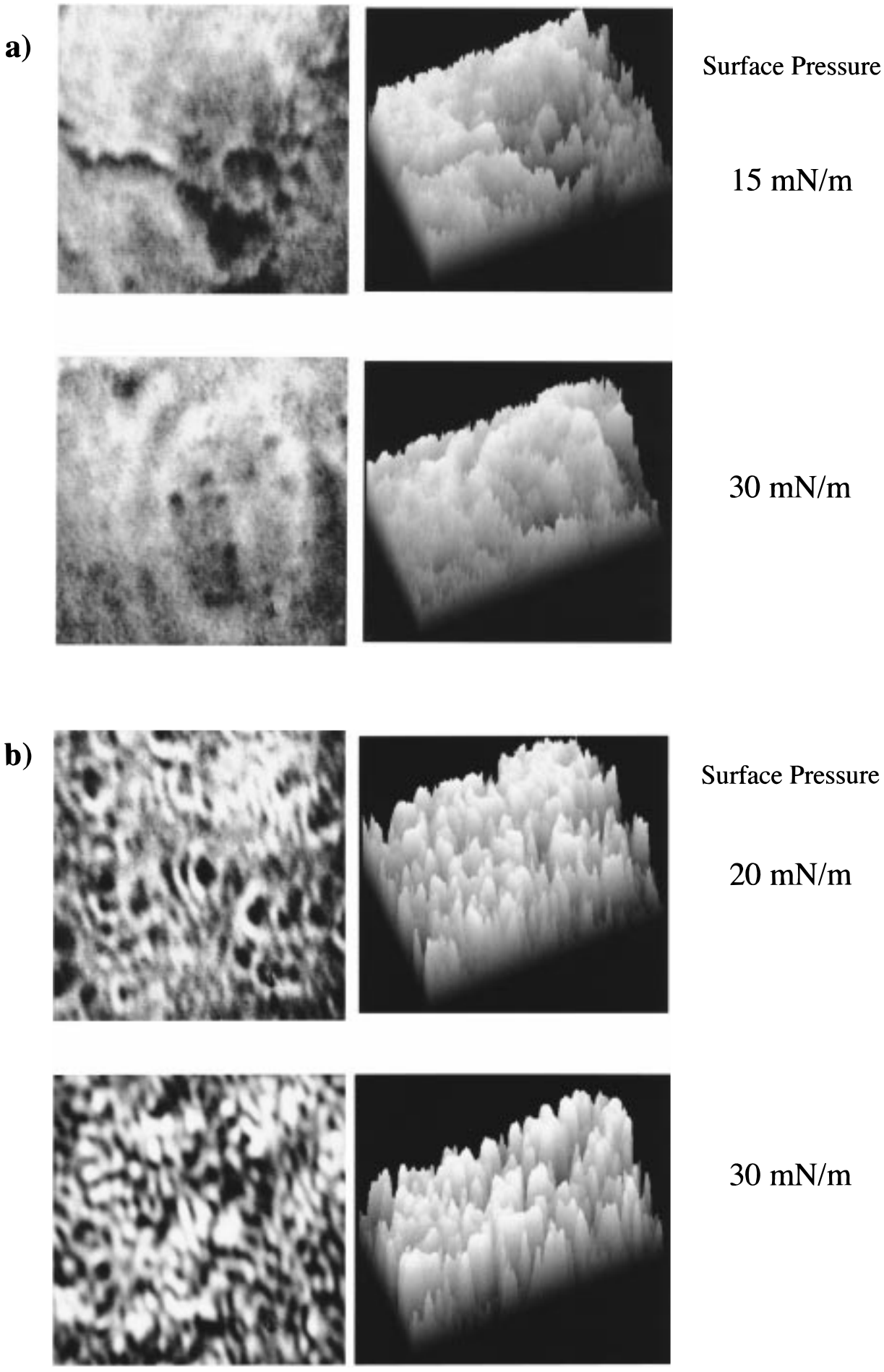
a)
Surface Pressure
15 mN/m
30 mN/m
b)
Surface Pressure
20 mN/m
30 mN/m

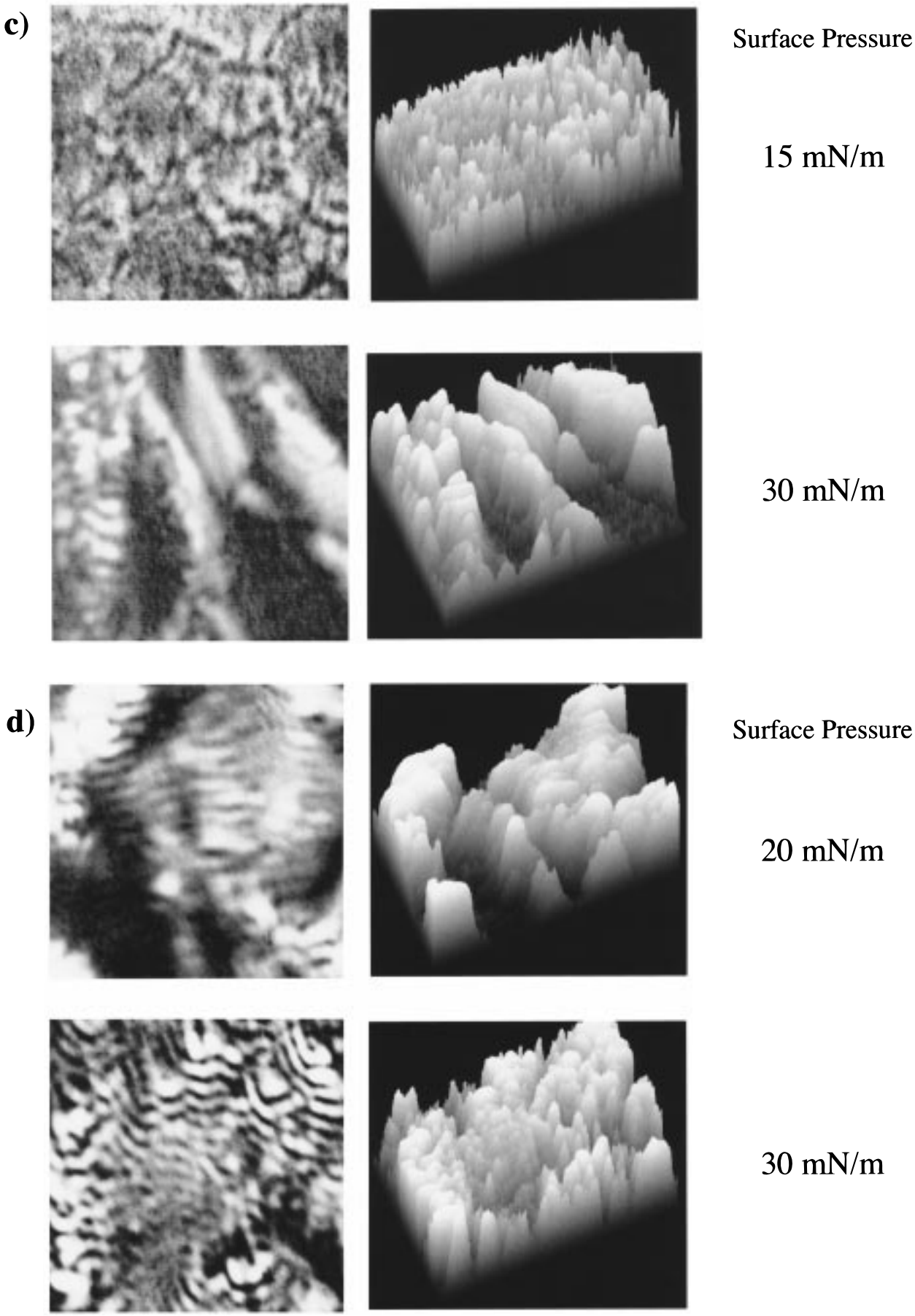

Figure 5. Brewster angle images (left column) and their 3-D representations (right column) recorded during the compression of the $2C_{18}TAZ$ monolayer with different complementary hydrogen bonding additives in the subphase: (a) pure water; (b) BA 10 mM; (c) BT 10 mM; (d) CA 10 mM.

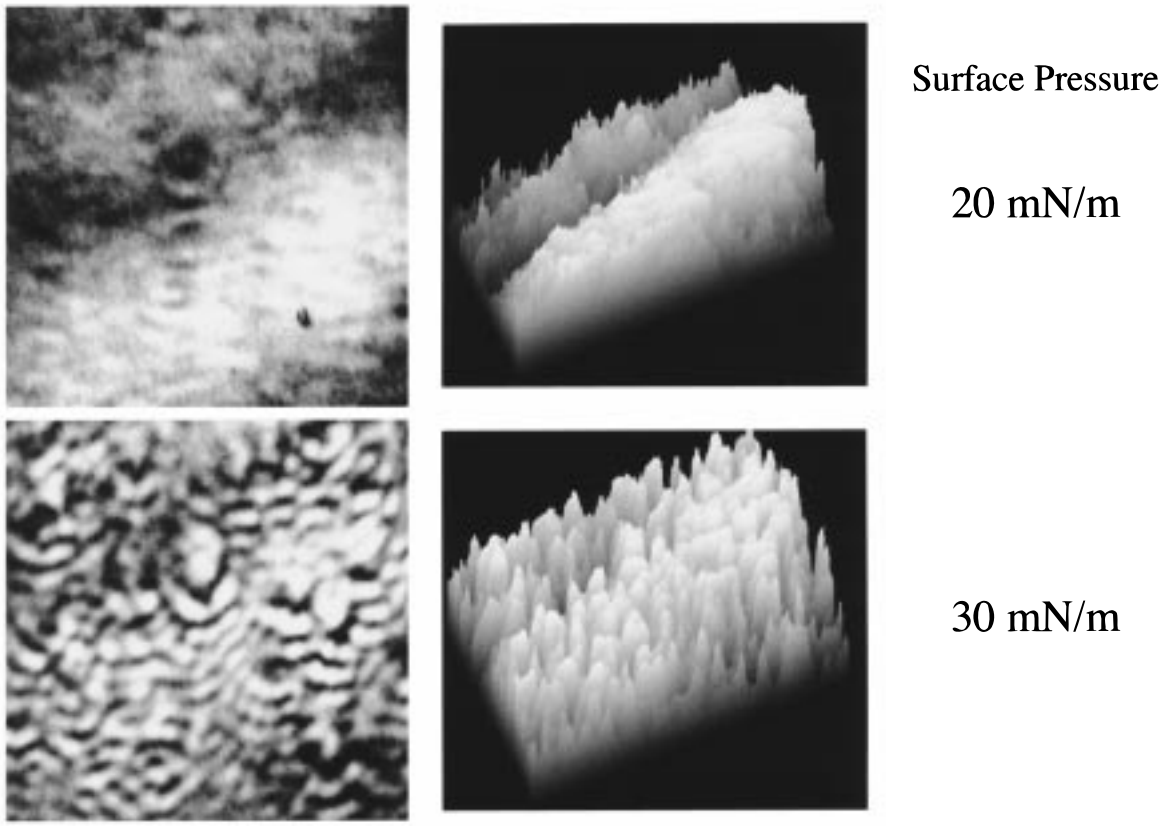

Figure 6. Brewster angle images (left column) and their 3-D representations (right column) recorded during the compression of the $2C_{18}$TAZ monolayer in the BA subphase (10 mM) with the addition of 20% DMSO to water.

However, hydrogen bonding is not the only possibility. Since the headgroup of the $2C_{18}$TAZ molecule is an aromatic ring, the $2C_{18}$TAZ molecules at the air−water interface can be more tightly packed due to the $\pi-\pi$ stacking effect. Especially when the $\pi-\pi$ stacking direction is along the moving direction of barrier, certainly the limiting area will decrease. On the basis of this study it is not clear whether hydrogen bonding, $\pi-\pi$ stacking, or both work together at the same time to affect the $2C_{18}$TAZ monolayer structure.

Effect of Different Complementary Hydrogen Bonding Additives in the Subphase to the Structure and Properties of $2C_{18}$TAZ Monolayer. As pointed out in the Introduction, the complementary hydrogen bonding between disubstituted TAZs and barbiturates or cyanurates has been carefully studied in solution and solid state. It seems there is no fundamental difference for the binding mode between BA, BT, and CA with the same TAZs. Only by changing the steric properties of the substituent group on TAZs, three motifs have been observed for the self-assemblies. However this seems not to be the case at the air−water interface.

Starting with the comparison between BA and CA subphase, the BA subphase led to obvious changes for the $\pi-A$ isotherm while the CA subphase only decreased the collapse surface pressure. As previously discussed, the surface morphologies of the $2C_{18}$TAZ monolayer in pure water, BA subphase, and CA subphase shown in BAM images (parts a, b, and d of Figure 5, respectively) are also quite different. The observation of very bright "strips" in the BA subphase (Figure 5b) strongly suggests the formation of a hydrogen bonded network between the $2C_{18}$-TAZ monolayer and the BA molecules from subphase. The occurrence of a highly organized $2C_{18}$TAZ monolayer in the CA subphase (Figure 5d) also clearly indicates the profound effect of CA on the $2C_{18}$TAZ monolayer. Originally the interpretation for the isotherm obtained from the CA subphase suggested that the CA molecule did not bind to the $2C_{18}$TAZ monolayer efficiently because the limiting molecular area remained nearly unchanged. It was mentioned in Rinsdorf's work that the $\pi-A$ isotherms of a barbituric acid lipid on a water and TAP subphase (0.1 mM) at pH = 3.0 are almost identical but with slightly differing collapse surface pressures.[41] This system was found to catalyze the hydrolysis of barbituric acid lipids highly efficiently. This contradiction was explained as the complementary tight binding of two components at the air−water interface. The BAM images presented here strongly support this interpretation. All the experimental results direct our thoughts to the direction that, instead of forming weak hydrogen bonding within the $2C_{18}$TAZ monolayer, the CA molecules from the subphase formed a highly efficient complementary hydrogen bonded network with $2C_{18}$TAZ molecules at the air−water interface as shown in Figure 8a. The formation of this highly defined linear tapelike "supramolecule" at the air−water interface was soundly confirmed by the observation of long "striplike" structures in their BAM images (Figure 5d). The CA molecules were inserted between $2C_{18}$TAZ molecules so perfectly, even by rough estimation, the insertion should not be expected to affect the molecular area of the $2C_{18}$TAZ monolayer significantly. This point was further clarified by molecular modeling[50] of the hydrogen bonding network formed from the $2C_{18}$TAZ monolayer and CA subphase (Figure 9). From the side view of the network, it is shown that the distance between two alkyl chains of the $2C_{18}$TAZ molecule is about 6.5 Å, while the distance between two carbonyl oxygens of CA molecules in the network is approximately 10 Å, which means the two alkyl chains from two adjacent $2C_{18}$TAZ molecules (separated by one CA molecule) are too close to each other. To release the steric repulsion, the two alkyl

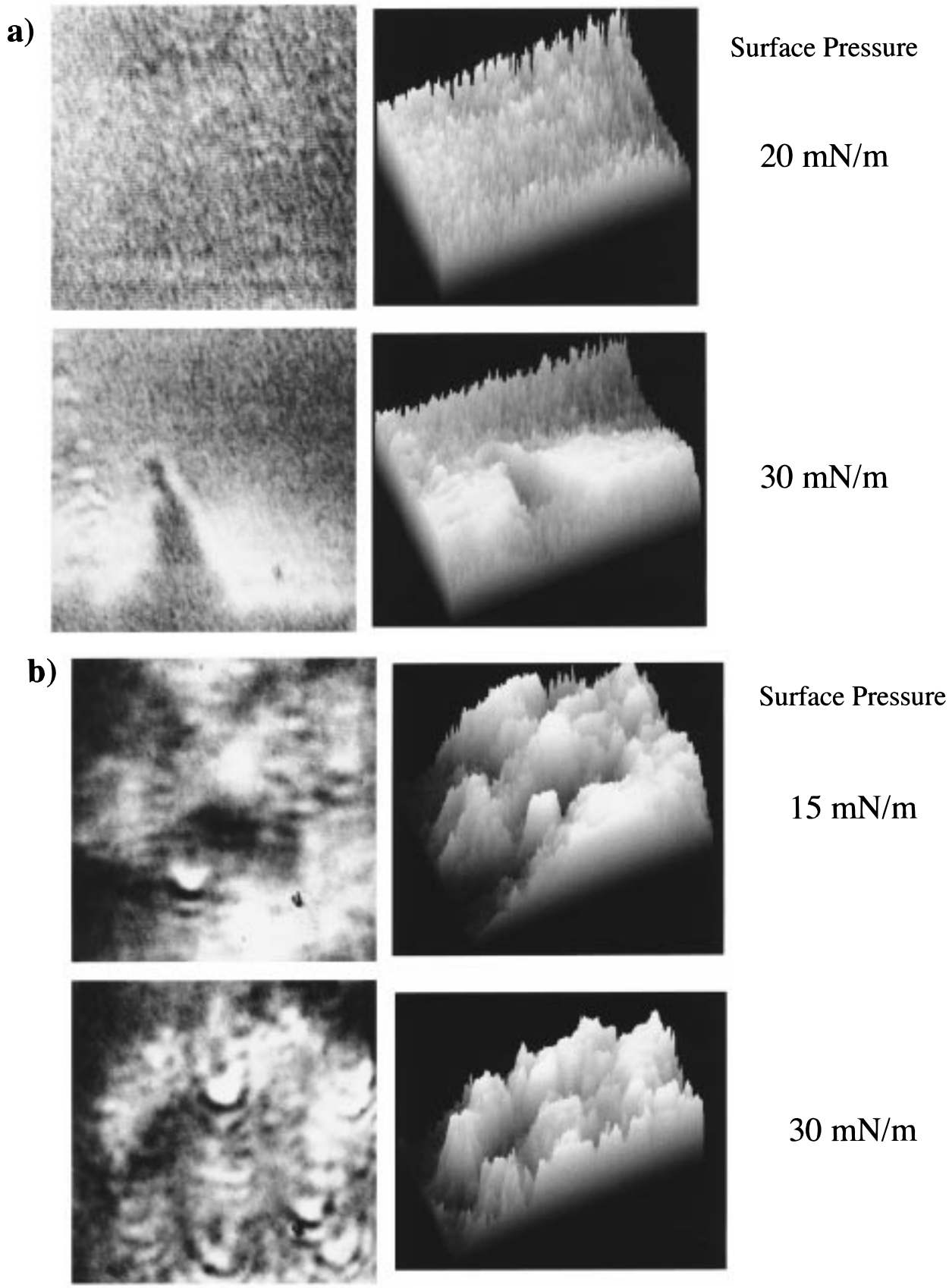

Figure 7. Brewster angle images (left column) and their 3-D representations (right column) recorded during the compression of the $2C_{18}$TAZ monolayer in CA subphase (10 mM) with the addition of (a) 10% DMSO and (b) 10% dioxane.

chains from the $2C_{18}$TAZ molecule have to be tilted from the two alkyl chains in the adjacent $2C_{18}$TAZ molecule, as it is shown in the top view of the model. This slightly "squeezed" structure explains perfectly why the molecular area obtained from the CA subphase is even smaller than the one from the pure water subphase.

Even though from their BAM images it is clearly shown that the BA molecules have a strong effect on the $2C_{18}$-

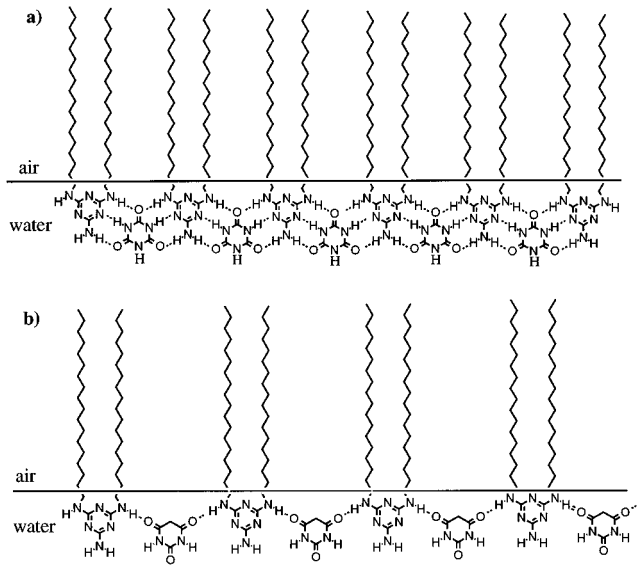

Figure 8. (a) Schematic representation of the formation of the hydrogen bonding network at the air−water interface from the binding of the $2C_{18}$TAZ amphiphile with its complementary component CA by six-point hydrogen bonding. (b) An illustration of possible two-point hydrogen bonding network formed from the binding of BA to the $2C_{18}$TAZ monolayer.

TAZ monolayer, it is not clear if the BA molecules from the subphase formed a 1:1 hydrogen bonded network with the $2C_{18}$TAZ monolayer as CA did. In other words, if the BA molecules also formed a 1:1 ratio hydrogen bonded network with the $2C_{18}$TAZ amphiphile as shown in Figure 8a, results similar to those obtained from the CA subphase would be expected. The molecular area should not change significantly and the BAM images should also be similar. The experiments afforded the opposite results. The only explanation for this contradiction is that BA molecules did not bind with $2C_{18}$TAZ amphiphile solely in the same complementary mode by six-point hydrogen bonding. In fact, there are at least three other possibilities for BA binding with $2C_{18}$TAZ headgroups by hydrogen bonding (Figure 8b). These other binding modes increase the molecule area of the $2C_{18}$TAZ monolayer. Even though in Kunitake's work, by FT-IR, XPS, or AFM images analysis, etc., it is claimed that BA molecules form a 1:1 hydrogen bonded network with dialkylTAZ amphiphiles, none of the experimental results can tell whether BA molecules bind with $2C_{18}$TAZ molecules by two-point, four-point, or six-point hydrogen bonding.[48] In all these possibilities it was possible to see the shift of IR peaks of the carbonyl groups from BA and N−H groups from TAZs. Independent of two-point, four-point, or six-point hydrogen bonding, they all can form 1:1 assembled networks at the air−water interface. Similar results can be found in Rinsdorf's work which studied the binding of TAP and urea to barbiturates amphiphiles.[49] If TAP was inserted into BA lipids in a way similar to that shown in Figure 8a, the limiting molecular area of BA lipid should not increase as much as the $\pi-A$ isotherms show.

From a thermodynamic point of view, the six-point hydrogen bonding network should be more stable than any other binding motif in solution. The formation of one hydrogen bond lowers free energy about 1−5 kcal/mol. However, the situation at the air−water interface is not as simple. Except for the possibility of forming oligomers by hydrogen bonding in solution or at the air−water interface, even for BA monomers, there are at least two possible orientations: if we call the carbonyl group between two amides as the "head", then it can stay at interface either "head" up or "head" down. In case of "head" up, the BA molecule will be able to insert to the $2C_{18}$TAZ monolayer by six-point hydrogen bonding as shown in Figure 8a. But if the "head" is down, then BA molecule can optimally use only two hydrogen bonding between adjacent $2C_{18}$TAZ molecules (Figure 8b), with the other hydrogen bonding sites being solvated by other polar molecules. This binding mode definitely will increase molecular area. In summary, the existence of multiple binding mode of BA to the $2C_{18}$TAZ monolayer results in an increase of molecular area and inhomogeneity of their BAM images (Figure 5b). With respect to CA, because of its C_3 symmetry, there is no difference about how it orients itself at the air−water interface. Only by adjusting itself very slightly is it always possible for CA to reorient so it can be inserted to the $2C_{18}$TAZ monolayer to form a six-point hydrogen bonded network as shown in Figure 8a. Since the formation of the hydrogen bonded network is more homogeneous, evenly scattered long "strip" structures are observed in their BAM images (Figure 5d). The different structures of hydrogen bonding components in the solution or at the air−water interface have a significant effect on their binding mode with $2C_{18}$TAZ monolayers, which consequently results in different changes on the $2C_{18}$TAZ monolayer $\pi-A$ isotherms and surface morphologies.

Compared to BA, BT has replaced the two non-imide hydrogens with two ethyl groups. We expected the effect of BT in the subphase to the $2C_{18}$TAZ monolayer should be more or less similar to that of BA. Because of the steric and hydrophobic property of the ethyl group, the binding of the BT molecule to the $2C_{18}$TAZ monolayer should also be weaker than that of BA. The $\pi-A$ isotherm seems to confirm this assumption. The shape of the isotherm is very close to the one from the BA subphase, but the changes compared to the $\pi-A$ isotherm from water are much less than the changes brought by the BA subphase (Figure 2). From its BAM images (Figure 5c), one can see brightness of the area is much less intense than the images from BA subphase at similar surface pressures, which means the molecular density at the air−water interface is lower. During the compression there are also some bright long "strips" formed which indicate the formation of highly organized structures. These experimental results support that BT binds with $2C_{18}$TAZ monolayer in a similar way, but more weakly than BA.

Effect of DMSO and Dioxane on the Hydrogen Bonded Networks Formed by $2C_{18}$TAZ Amphiphile and BA or CA at the Air−Water Interface. As previously mentioned, the addition of DMSO did not bring much change to the $\pi-A$ isotherm of the $2C_{18}$TAZ monolayer in the pure water subphase (Figure 3a). The slightly lower collapse surface pressure is probably due to the solvation of the monolayer by DMSO. With the addition of 10% dioxane, the molecular area is slightly decreased and the collapse surface pressure is more obviously decreased (Figure 3a). 1,4-Dioxane is a nonpolar solvent highly miscible in water. The dioxane molecules serve to extract the water molecules surrounding the $2C_{18}$-TAZ headgroups, bringing $2C_{18}$TAZ molecules closer to each other to form an even more tightly packed monolayer. In BA subphase, the addition of DMSO has a significant effect on the $\pi-A$ isotherms (Figure 3b). With an increasing percentage of DMSO in the subphase, the $\pi-A$ isotherms become more like the $\pi-A$ isotherm from pure water. Due to the strong solvating ability of DMSO on BA, the oligomerization of BA by hydrogen bonding is partially disrupted. BA is then distributed in the subphase and at the air−water interface more evenly, which means

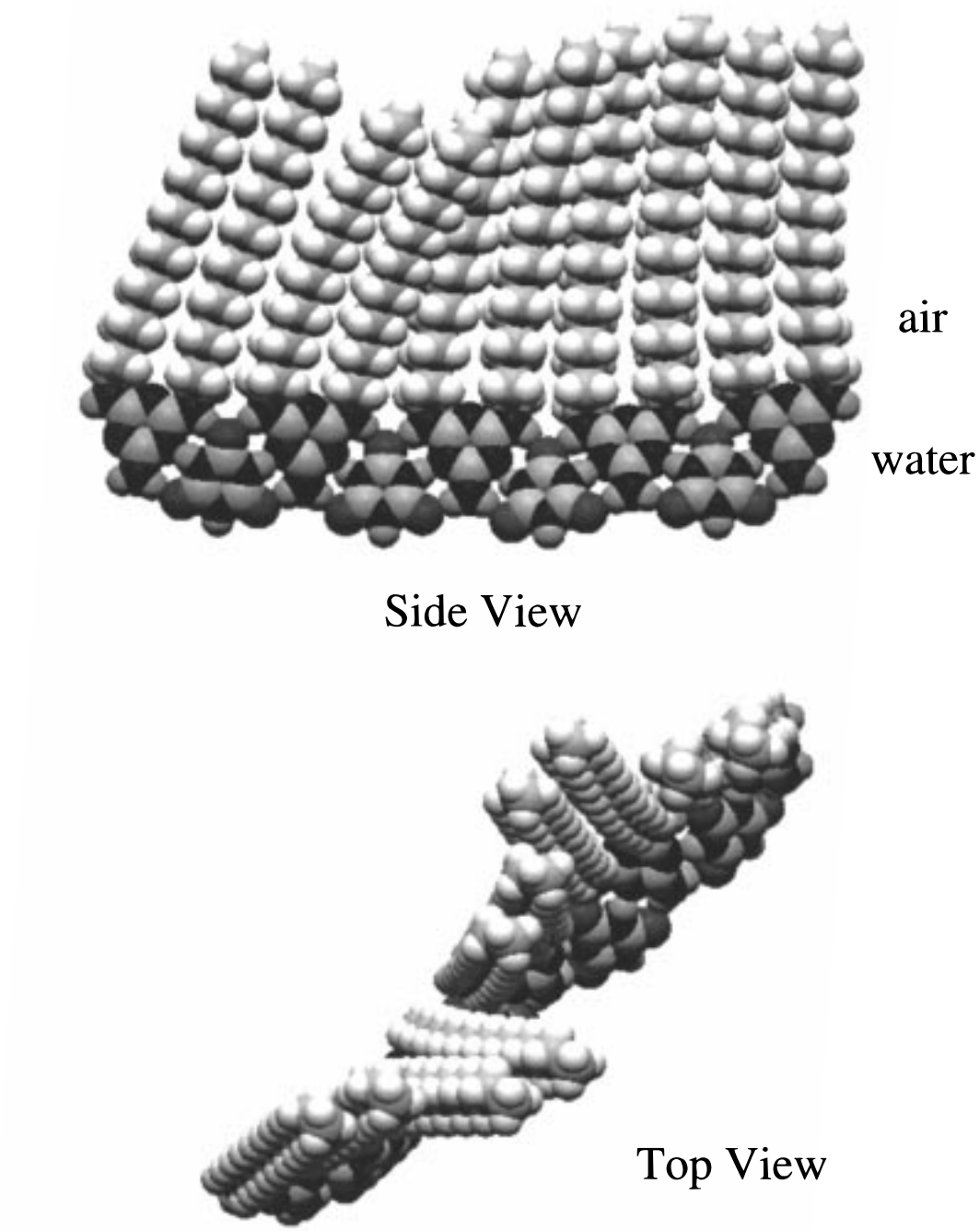

Figure 9. Top view and side view of the macromodel structure of a 1:1 hydrogen bonded network formed from the $2C_{18}$TAZ amphiphile and CA at the air−water interface. The distance between two carbonyl oxygens of adjacent CA molecules is approximately 10 Å. The distance between two alkyl chains of $2C_{18}$TAZ is about 6.5 Å. The calculated limiting molecular area of $2C_{18}$TAZ based on this model is 50.4 Å^2/molecule.

the "local" concentration of BA is decreased. Following this, the hydrogen bonding between BA and $2C_{18}$TAZ is partially disrupted and becomes more homogeneous. The BAM images of the $2C_{18}$TAZ monolayer in BA subphase with the addition of 20% DMSO (Figure 6) is in strong agreement with the $\pi-A$ isotherm measurements. At a surface pressure of 20 mN/m, one can see a more plain and uniform surface structure compared to the one from the BA subphase without the addition of DMSO, which corresponds to a lower molecular density at air−water interface.

The difference between 10% DMSO and 10% dioxane on the $2C_{18}$TAZ monolayer in the CA subphase has also been analyzed. Even though the changes are subtle, trends through their $\pi-A$ isotherms (Figure 3c) and Brewster angle images (Figure 7a,b) can clearly be seen. As expected, the addition of 10% DMSO disrupts the hydrogen bonding between amphiphile and CA molecules. The solvation of CA molecules in subphase and at the air−water interface makes the formation of the hydrogen bonded network even more homogeneous, as was verified by their less dynamic surface morphologies from BAM images in Figure 7a. In contrast, the rough surface morphologies with the addition of 10% dioxane to the subphase (Figure 7b) can be attributed to a physical property of dioxane. The nonpolar structure still has two oxygen atoms in the six-membered ring. This makes dioxane a poor solvent for polar molecules while maintaining good solublility in water by hydrogen bonding. It strengthens the hydrogen bonding network by removing

water molecules surrounding the CA and $2C_{18}$TAZ molecules so they have more chance to bind with each other by hydrogen bonding.

Conclusion

The structure and properties of a $2C_{18}$TAZ monolayer on different subphases, which include pure water and subphases containing different hydrogen bonding components, have been studied. Surface pressure−area isotherm measurements, UV−vis absorption spectra at the air−water interface, and Brewster angle microscopy have been employed in this work. For the first time we have found that the $2C_{18}$TAZ amphiphile forms an irreversible monolayer at the air−water interface through "autoassembly". The binding of BA molecules to the $2C_{18}$TAZ monolayer can be detected by UV spectroscopy at subphase concentrations as low as 0.01 mM. Different hydrogen bonding components have different effects on the structure and properties of the $2C_{18}$TAZ monolayer, and these different effects are probably due to the existing structures of hydrogen bonding components at the air−water interface. The observation of long "striplike" structures from their Brewster angle images at the BA, BT, and CA subphase clearly indicates the formation of highly organized hydrogen bonding networks at the air−water interface. The effect of organic solvents in subphase on the $2C_{18}$TAZ monolayer has also been investigated. The strong solvating ability of DMSO disrupts the hydrogen bonding network, whereas the poor solvating ability of dioxane enhances the hydrogen bonding between $2C_{18}$TAZ monolayer and its hydrogen bonding complements.

LA971329+